IOP Conf. Series: Materials Science and Engineering **192** (2017) 012031 doi:10.1088/1757-899X/192/1/012031

Prediction of steel corrosion resistance based on EBSD-data analysis

D S Chezganov, M A Borovykh and O A Chikova

Ural Federal University, Ekaterinburg, 620000, Russian Federation

E-mail: chezganov.dmitry@urfu.ru, chik63@mail.ru

Abstract. We experimentally compared the samples of chromium-manganese steel prepared with various heat-treatment modes to predict the corrosion resistance of the steel relative to hydrocarbon influence. The study was done using scanning electron microscopy, X-ray energy dispersive spectroscopy and electron backscattered diffraction. The surface visualization and elemental analysis allowed to reveal the existence of inclusions and discontinuities and their elemental composition. The peculiarities of crystal structure, grain sizes and orientations were revealed by the analysis of misorientation distribution histograms, and orientation, band contrast and Schmidt factor maps. The analysis allowed to conclude which of the heat-treatment modes provides the increase of corrosion resistance relative to the hydrocarbons influence.

1. Introduction

The corrosion resistance is the important characteristic of the modern functional materials. The preliminary estimation of the material corrosion resistance is based on the study of its microstructure, phase composition and crystal structure. Detection and analysis of the material corrosion signs are usually realized by optical and electronic microscopy, X-ray phase analysis and measurement of micro hardness [1-3].

It is known that the low-energy and special boundaries of metallic grains have a high resistance to destruction [4-5]. The free energy of grain boundaries plays central role in boundary diffusion and segregation of impurity atoms [6]. The increase of a number of the low-angle special boundaries leads to raise of the metal corrosion resistance [7-8]. The analysis of diffraction patterns of backscattered electrons makes it possible to estimate the fraction of the low-angle and special (low-energy) grain boundaries of a metallic material, to construct a Schmidt factor (or Taylor factor) maps and a grain misorientation histograms (correlated distribution). The correlated misorientations display data between neighboring points. The analysis of grain misorientation histograms determines the fraction of the low-angle boundaries. The effects of the inhomogeneous stress-strain state, the criterions of the intergranular destruction of the metal materials based on analysis of Schmidt and Taylor factor maps are discussed in works [9-11].

In this work, we presented an analysis of capabilities of electron backscattered diffraction (EBSD) method for the prediction of the steel corrosion resistance relative to the hydrocarbon influence. The study of microstructure and crystal structure of samples was made to optimize the heat treatment mode.

2. Materials and experiment

The comparative analysis of EBSD data obtained for different samples cut from metal pipes made of chromium-manganese steel and heat-treated by various methods was made. The studied chromium-manganese steel contained components in following ratio [11-12] (Table 1):

Table 1. Components of studied chromium-manganese steel.

Component	Content, weight%
Carbon	0.31-0.38
Silicon	0.17-0.37
Manganese	0.95-1.25
Chromium	1.0-1.30
Vanadium	< 0.06-0.12
Sulfur	< 0.035
Phosphorus	< 0.035

The samples were selected from ready-made pipes at the "Sinarskiy trubnyy zavod" (Sinarskiy pipe plant) and differed from each other by heat treatment mode: Sample 1 - normalization at 910 °C and high-speed tempering at 700 °C in the furnace; Sample 2 - high-speed tempering at 700 °C in the furnace; Sample 3 - normalization at 910 °C; Sample 4 - long tempering at 700 °C.

Before study the sample surfaces were grinded and polished by diamond abrasive down to 1 μm and colloidal silica during 20 min at the final stage.

The sample surfaces were studied by the three methods: (1) scanning electron microscopy (SEM), (2) X-ray energy dispersive spectroscopy (EDS) and (3) EBSD. The study was made by scanning electron microscope AURIGA CrossBeam (Carl Zeiss, Germany) equipped with the EBSD analysis system HKL Channel 5(Oxford Instruments, UK) with spatial resolution down to 20 nm and EDS system IncaEnergy (Oxford Instruments, UK) with 350X-MAX X-ray detector with spatial resolution about 1 μm and spectral resolution of 125 eV at Kα line of Mn.

The SEM was used for visualization of surface morphology and structural defects in secondary electron mode with the resolution down to 2 nm. The EDS was applied for revealing of elemental composition of defects and inclusions. The EDS data collection and processing were made by means of IncaEnergy software.

The EBSD was used for detailed study of structural state of the sample surface. The EBSD data acquisition was made by Flamenco Acquisition software (Oxford Instruments, UK). The accelerating voltage of 20 kV and electron beam current of 8 nA were used during scanning. The areas with a size of 20×20 μm^2 were scanned with a step size of 80 nm. The obtained data was processed and analyzed by Tango software (Oxford Instruments, UK). The band contrast (BC) map with coincident site lattice boundaries (CSL), Schmidt factors maps and histograms of misorientation angle distribution were constructed. The histograms consist of 2000 columns with width of 0.3^o. The angle of tolerance was chosen to be 5^o.

3. Results and discussion

The reason of the intergranular corrosion for ferrites steels, such as chromium-manganese steel, is an emergence of local distortion of crystal lattice and presence of large-angle non-special grain boundaries. The appearance of local or pitting corrosion relates to localization of the non-metal inclusions such as the oxides of iron, silicon and aluminum. This was a reason for selection of regions for EBSD-study associated with metal defects of technological origin, e.g. the cracks filled with gas or dross.

The study of the surface by SEM allowed to reveal existence of inclusions and discontinuities with sizes about 1-10 μm in subsurface layer of the pipes. The EDS analysis showed oxygen content in the inclusions. Moreover, the increased of carbon content in surface layer was found. The elemental analysis of the inclusions revealed a presence of Fe, Mn, Si, Cr, Al, O and C. The systematic

segregation of atoms wasn't found. The extended non-metal inclusions with the size about 50 μm were observed in the sample 2, which was oriented into the pipe depth. In sample 4 the non-metal inclusions demonstrated spherical shape and size about 1 μm. It was supposed that these inclusions consist of aluminum oxide Al_2O_3.

The figures 1(a) – 1(d) represents the BC maps with superimposition of colored CSL boundaries. The colors are coded by CSL type as shown in the histogram of CSL boundaries distributions (Fig. 1(e) – (1(h)). The band contrast is an EBSD pattern (EBSP) quality factor derived from the Hough transform that describes the average intensity of the Kikuchi bands with respect to the overall intensity within the EBSP[13]. The values are scaled to a byte range from 0 to 255 (i.e., low to high contrast). With this scale mapped to a grayscale from black to white, image-like maps can be plotted. These "images" show the microstructure in a qualitative fashion that were used to seeing either in the SEM or light microscope. Because EBSPs along grain boundaries tend to show poor BC they appear dark in a map. Conversely, EBSPs in undeformed regions of a grain appear light.

It was observed that the sample 3 have the smallest grains which might indicate to greater plasticity and corrosion resistance of this sample (Fig. 1(c)). The revealed orientation distribution demonstrated the wide range of colors close to discontinuities which indicated a high degree of grain misorientations and weakly pronounced metallographic texture.

The revealed CSL boundaries, close to Brandon's criterion for special boundaries, marked by light colored lines while other grain boundaries were kept in the form of dark lines. CSL boundaries are the special boundaries which fulfil the coincident site lattice criterias whereby the lattices are sharing some lattice sites. CSLs are characterized by Σ where Σ is the ratio of the CSL unit cell compared to the standard unit cell. CSL boundaries typically have a significant impact on the material properties, which means that from a materials engineering viewpoint it is important to determine both the ratio of CSL boundaries and their distribution within the material.

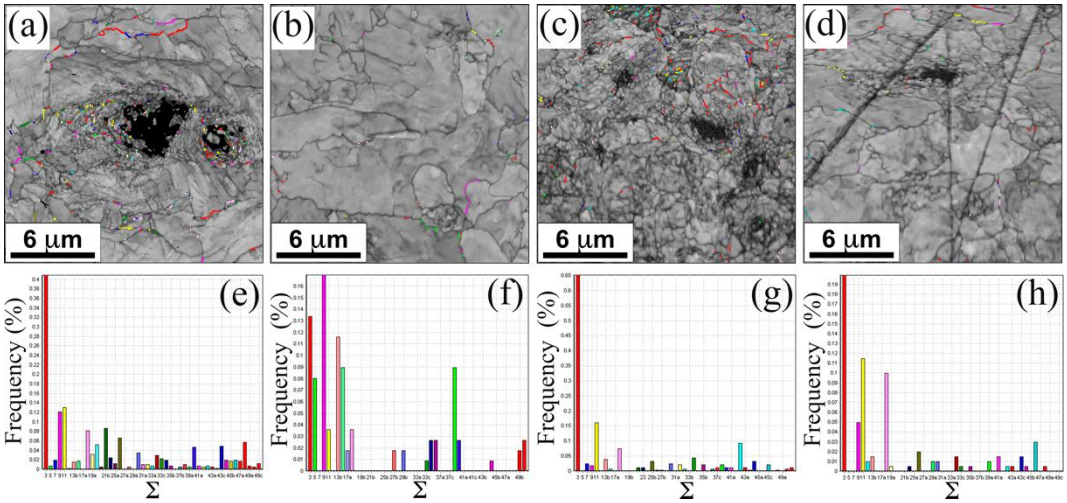

Figure 1. (a) – (d) Band contrast maps with colored CSL boundaries obtained at different samples: (a) 1, (b) 2, (c) 3, (d) 4. (e) – (h) CSL boundaries distributions and color code for sample: (e) 1, (f) 2, (g) 3, (h) 4.

The "dark" grain boundaries form a continuous network while twin boundaries do not form one. With all the differences in the location of twin grain boundaries their relative proportion are about the same for all samples. All the twins are inside the grains and do not cross the grain boundaries. It means that they arose after a common grain structure was formed during rolling process. The revealed twins are the annealing twins. The part of special boundaries is small (~ 1.5-2.0%) and the largest number of them in the microstructure of the sample 4 (Fig. 1(d)), which indicates its higher corrosion resistance [14-15].

The Figure 2 shows the histograms of misorientation angle distribution. The uncorrelated misorientations (light gray lines) indicate misorientations between randomly selected points in the data set. Correlated misorientations (dark gray lines) display data between neighboring points, in the other words, the angle distribution of the grain boundaries. A theoretical curve (solid black curve) shows what one would expect from a random set of orientations. The difference between uncorrelated misorientation and the theoretical curve arises, as a rule, due to the strong texture, which revealed itself in all samples (Fig. 2). According to this fact, the highest texturing was revealed in sample 2 (Fig. 2b). The presence of a larger specific fraction of low-angle boundaries is the most pronounced for sample 3, which indicates its high plasticity and corrosion resistance (Fig. 2(c)).

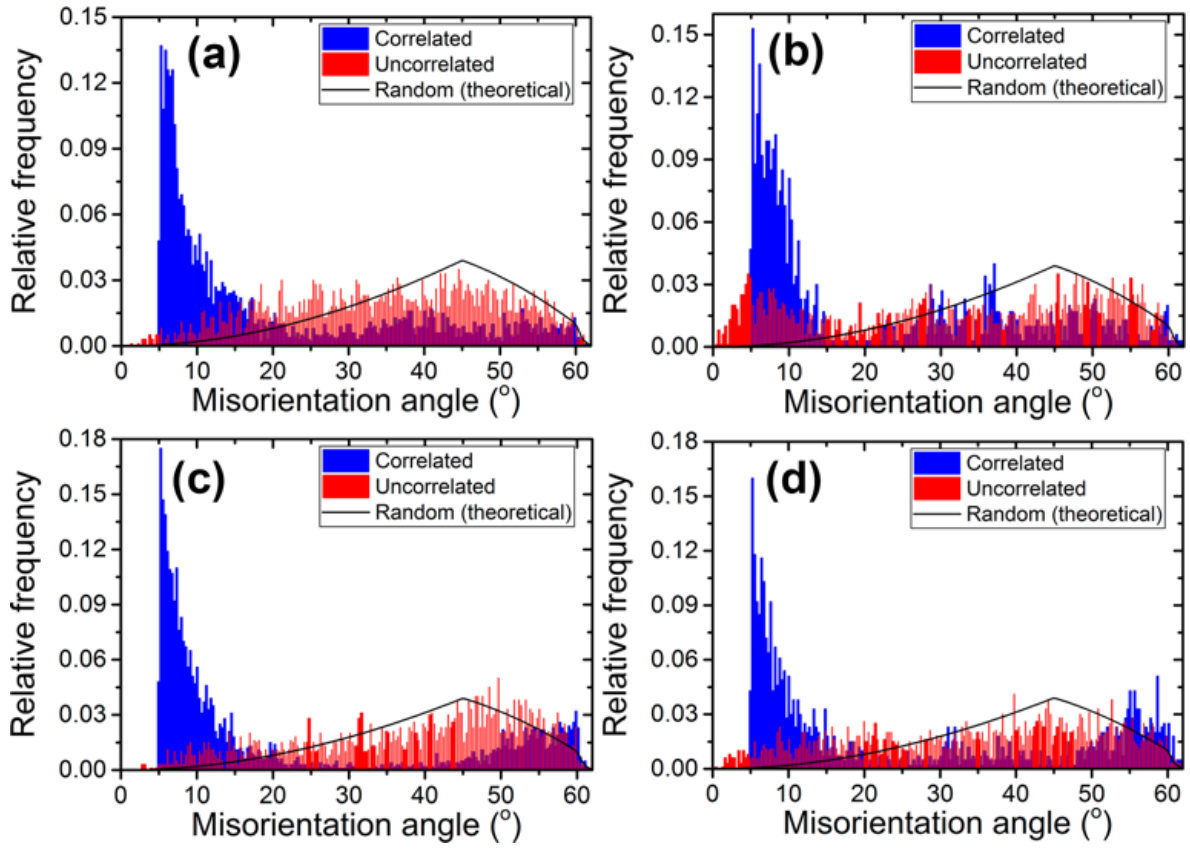

Figure 2. Misorientation angle distribution shows the frequency of grain boundaries in the sample: (a) 1, (b) 2, (c) 3, (d) 4.

The Schmidt factor maps are used to determine the uniformity degree of possible deformation. In the presence of an external load, for example, during operation, deformations begin to develop in light grains and gradually move to dark ones. In external mechanical loading in cubic crystals with a bcc lattice type, such as α-Fe, plastic deformation by slipping can take place.

The Schmidt factor maps were constructed for a slip system typical for BCC crystals: {110} <111> with loading direction parallel to OZ axis. The Fig. 6 demonstrated that there is a wide range of shades of gray close to the discontinuities due to local distortions of the crystal lattice of the metal, which indicates a low deformation uniformity of the metal and a high probability of the pitting corrosion. The Schmidt factor map for sample 3 is characterized by the greatest deformation uniformity, which is an indirect evidence of its greater resistance to intercrystalline corrosion.

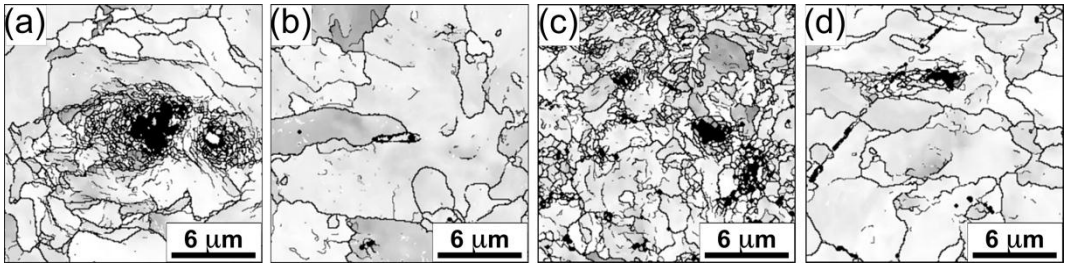

Figure 3. Schmidt factor maps for sample: (a) 1, (b) 2, (c) 3, (d) 4.

4. Conclusion

The comparative study of different samples cut from metal pipes made of the chromium-manganese steel and heat-treated by various methods was made by SEM, X-ray EDS and EBSD to predict the corrosion resistance of steel relative to the hydrocarbon influence. SEM surface visualization revealed the existence of inclusions and discontinuities with sizes about 1 – 50 μm. The EDS analysis showed oxygen content in the inclusions and elevated content of carbon in the surface layer. The EBSD analysis allowed to reveal peculiarities of crystal structure, grain sizes and orientations and obtain the data of local mechanical stresses. We have shown that the heat treatment mode influences on the grain size, misorientation distribution and Schmidt factor map. The analysis of EBSD-data allowed to conclude that heat-treatment mode for sample 3 provides the increase of the corrosion resistance relative to the hydrocarbons influence.

5. References

[1] Latanision R M 1995 *Corrosion* **51** 270
[2] Jargelius-Pettersson R F A 1998 *Corrosion* **54** 162
[3] Bell T 2002 *Surf. Eng*. **18** 453
[4] Watanabe T 1984 *Trans. Jap. Inst. Metals* **27** 73
[5] Watanabe T 1993 *Mater. Sci. Eng.: A* **166** 11
[6] Gupta G, Ampornrat P, Ren X, Sridharan K and Allen T R Was G S 2007 *J. Nucl. Mater.* **361** 160
[7] Lin P, Palumbo G, Erb U and Aust K T 1995 *Scr. Mater.* **33** 1387
[8] Palumbo G, King P J, Aust K T, Erb U and Lichtenberger P C 1991 *Scr. Mater.***25** 1775
[9] Watanabe K, Matsuda K, Miura N, Uetani Y, Ikeno S., Yoshida T and Murakami S 2014 *Keikinzoku/Journal of Japan Institute of Light Metals* **64** 368
[10] Lopatin N V 2012 *Mater. Sci. Eng.: A* **556** 704
[11] Zhou W and Wang Z L 2007 *Scanning microscopy for nanotechnology: techniques and applications* (New York: Springer) 522
[12] Lin P, Palumbo G, Harase J and Aust K T 1996 *Acta Mater.* **44** 4677
[13] Chun H, Na S M, Mudivarthi C and Flatau A B 2010 *J. Appl. Phys.* **107** 09A960

Acknowledgments

The equipment of the Ural Center for Shared Use “Modern nanotechnology” UrFU was used.